Binding of Substance P Agonists to Lipid Membranes and to the Neurokinin-1 Receptor†

Anna Seelig,*,‡ Thomas Alt,‡ Sandra Lotz,‡ and Günter Hölzemann§

University of Basel, Klingelbergstrasse 70, CH-4056 Basel, Switzerland, and Merck KGaA, D-64271 Darmstadt, Germany

Received October 11, 1995; Revised Manuscript Received February 1, 1996⊗

ABSTRACT: Three new analogues of the neuropeptide substance P (SP) were synthesized. The C-terminal message segment was made more hydrophilic in (Arg^9)SP or more hydrophobic in (Nle^9)SP. In ($AcPro^2$, Arg^9)SP the charge at the N-terminal address segment was reduced, while that of the message segment was increased. The rationale underlying these substitutions was to correlate the physical-chemical properties of the SP-analogues, in particular their lipid-induced conformation and membrane-binding affinity, with receptor binding and functional activity. In solution, all three analogues exhibited random coil conformations as evidenced by circular dichroism spectroscopy. Addition of SDS micelles induced partially α-helical structures. The same structure was also produced by negatively charged lipid vesicles for ($AcPro^2$, Arg^9)SP and (Arg^9)SP whereas both α-helix-like structures and *β*-sheet structures were observed for SP and (Nle^9)SP. The measurement of the Gibbs adsorption isotherms and monolayer expansion studies provided quantitative data on the surface area requirement and on the membrane penetration area of the SP analogues. The thermodynamic parameters for lipid binding were determined with monolayer expansion measurements and high-sensitivity titration calorimetry. The apparent binding constants, K_{app}, for membranes containing 100% POPG were of the order of 10^3-10^5 M^{-1}. The binding was due to electrostatic attraction of the cationic peptides to the negatively charged membrane surface. The intrinsic (hydrophobic) binding constants, obtained after correcting for electrostatic effects, were much smaller with $K_p = 10 \pm 1$ M^{-1} for (Arg^9)SP, 9 ± 1 M^{-1} for ($AcPro^2$, Arg^9)SP, and 39 ± 3 M^{-1} for (Nle^9)SP. The measurement of the binding affinities to the NK-1 receptor and of the *in vitro* activities showed that all three peptides behaved as agonists. Their binding affinity to the neurokinin-1 receptor decreased with the size of the side chains at position 9 of the amino acid sequence but was independent of the cationic charge of the peptides. The fact that even the highly charged (Arg^9)SP has agonistic activity provides evidence that the binding epitope at the receptor is in a rather hydrophilic environment. This finding is in agreement with the low hydrophobic binding constants and the weak penetration of the three peptides into negatively charged membranes. It argues against a membrane mediated receptor mechanism and suggests that the agonist approaches the receptor binding site from the aqueous phase.

Substance P (SP),[1] R P K P Q Q F F G L M(NH_2), is widely distributed in the central and peripheral nervous system and in the gastrointestinal tissue (Nicoll et al., 1980) and is involved in various biological functions such as pain transmission and smooth muscle contractions (Regoli et al., 1989, 1994). SP binds preferentially to the G-protein coupled neurokinin-1 (NK-1) receptor consisting of seven putative transmembrane helices connected by variously large loops exposed to the extra- and intracellular aqueous phase. The binding site of SP and its agonists appears to involve residues of the first and second extracellular loop and of the second and seventh transmembrane domain, close to the extracellular membrane interface, as suggested by mutagenesis and heterologous expression experiments (Fong et al., 1992; Gether et al., 1993; Huang et al., 1994).

An address−message model has been proposed for SP such that its hydrophilic N-terminal region, or "address domain", is responsible for receptor selectivity whereas the hydrophobic C-terminal sequence, or "message domain", is responsible for triggering the receptor (Schwyzer, 1987). However, according to recent mutagenesis studies, "this model appears to be oversimplified when considered in the context of receptor interactions" (Huang et al., 1995). It was concluded by the same authors that "the address−message model needs to be modified to include the conformation factor."

SP and the NK-1 receptor represent one of the best studied peptide transmitter−receptor systems; however, it is still unclear whether peptide recognition occurs directly from the extracellular aqueous phase via collision with a surface-exposed binding site or whether it is mediated by the target membrane. The latter possibility was proposed on the basis of the amphiphilic properties of SP and its ability to change its conformation upon interaction with negatively charged interfaces (Rolka et al., 1986; Schwyzer 1991). On the other hand, lipid binding measurements of SP and (Sar^9, Met-$(O_2)^{11}$)SP, the latter being the most specific synthetic NK-1 agonist, have shown that the peptides have only a low affinity for the hydrophobic part of the bilayer, i.e., the binding to neutral membranes is weak whereas the binding to negatively

† Supported by Swiss National Science Foundation Grant 3100−42058.94.

* Corresponding author. FAX: +41-61-2672189.

‡ University of Basel.

§ Merck.

⊗ Abstract published in *Advance ACS Abstracts,* March 15, 1996.

[1] Abbreviations: SP, substance P; NK-1 receptor, neurokinin-1 receptor; POPC, 1-palmitoyl-2-oleoyl-*sn*-glycero-3-phosphocholine; POPG, 1-palmitoyl-2-oleoyl-*sn*-glycero-3-phosphoglycerol; SDS, sodium dodecyl sulfate; CD, circular dichroism spectroscopy; NMR, nuclear magnetic resonance spectroscopy.

0006-2960/96/0435-4365$12.00/0 © 1996 American Chemical Society

charged membranes is driven by the electrostatic attraction of the cationic peptides (Seelig & Macdonald, 1989; Seelig, 1992).

The primary goal of this work was to further clarify the binding properties of SP and to compare lipid binding with receptor binding and activity. To this purpose, three new SP derivatives, namely, (Nle^9)SP, (Arg^9)SP, and ($AcPro^2$, Arg^9)SP, were synthesized (Hölzemann et al., 1993). The message segment was made either more hydrophobic as in (Nle^9)SP or an additional positive charge was added as in (Arg^9)SP, or both message and address segment were altered as in ($AcPro^2$, Arg^9)SP. On the basis of our previous experience with SP and (Sar^9, $Met(O_2)^{11}$)SP it was expected that all three peptides should still behave as SP agonists.

A thermodynamic and conformational analysis of the SP-analogues in the presence of lipid membranes was performed by means of three physical-chemical techniques, revealing different aspects of the binding process. The change in the peptide conformation upon binding to lipid membranes was monitored by circular dichroism spectroscopy. The partial insertion of the peptide into the lipid head group region of a membrane was measured by means of the monolayer expansion method, while the heat change accompanying insertion was determined by high-sensitivity titration calorimetry. Finally, the agonistic properties of the three SP-derivatives were confirmed with binding assays to the NK-1 and NK-2 receptor and *in vitro* activity measurements.

Since the receptor binding site comprises amino acid residues of extracellular as well as of transmembrane segments, some of its amphiphilic properties are modeled by the also amphiphilic air−water or lipid−water interfaces. Even though a membrane-mediated receptor binding mechanism can be excluded, the conformation of the SP-agonists in the presence of amphiphilic interfaces probably bears a close resemblance to the receptor-bound conformation.

MATERIAL AND METHODS

Materials. SP (acetate salt) was purchased from Bachem (Bubendorf, Switzerland). Trifluoroacetate salts of (Arg^9)-SP, ($AcPro^2$,Arg^9)SP, and (Nle^9)SP were synthesized by solid phase methodology. A Millipore peptide synthesizer 9050 and the synthesis protocol supplied by the manufacturer were used. A 4-methylbenzhydrylamine resin was applied to obtain C-terminal amides, and the Fmoc group was used for N^{α} protection. The purity of the peptides was checked by HPLC, NMR, FAB-MS, amino acid analysis, and racemization tests and was >95%. The concentration of the peptide stock solution (5 mg of peptide per mL of deionized water) was determined by weight, taking into account the counterions. 1-Palmitoyl-2-oleoyl-*sn*-glycero-3-phosphocholine (POPC) and 1-palmitoyl-2-oleoyl-*sn*-glycero-3-phosphoglycerol (POPG) were purchased from Avanti Polar Lipids (Birmingham, AL).

Buffers. All measurements were performed at pH 7.4. For CD and monolayer measurements a 10 mM Tris-HCl buffer was used containing 154 mM NaF in the former case and 154 mM NaCl in the latter case. For calorimetry a phosphate buffer (50 mM KH_2PO_4/K_2HPO_4, 114 mM NaCl) was used since it was less temperature sensitive.

Vesicle Preparation. Small unilamellar vesicles composed of POPC, POPG and mixtures of the two were prepared by dissolving an appropriate amount of lipid in chloroform/methanol. The solvent was evaporated under a stream of nitrogen, and the lipid was dried under vacuum overnight. Buffer was added to the dry lipid film, and the suspension was vortexed extensively. The lipid dispersion was then sonified under nitrogen for 20−40 min (at 10 °C) until an almost clear solution was obtained. Metal debris from the titanium tip was removed by centrifugation in an Eppendorf centrifuge for 10 min.

Circular Dichroism Measurements. CD was measured with a Jasco J720 spectropolarimeter. All measurements were performed at room temperature. The path length of the cell was 1 mm. The spectra measured in the presence of sodium dodecyl sulfate (SDS) micelles or lipid vesicles were corrected by subtracting the spectra of corresponding SDS solutions or liposome dispersions. Results were plotted as mean residue ellipticity [Θ] in units of deg cm^2 $dmol^{-1}$.

Titration Calorimetry. Heats of reaction were measured with a Microcal OMEGA titration calorimeter (Microcal, Northhamton, MA) as described previously (Wiseman et al., 1989). Solutions were degassed under vacuum prior to use. The calorimeter was calibrated electrically. Measurements were performed at 28 °C. The data were evaluated using software developed by MicroCal.

Monolayer Measurements. A round Teflon trough designed by Fromherz (1975) (type RCM 2-T, Mayer Feintechnik, Göttingen, FRG), with a total area of 362 cm^2, divided into eight compartments was used. The trough was covered by a Plexiglas hood in order to keep a constant humidity. For the measurement of the Gibbs adsorption isotherms one compartment filled with 20 mL of buffer was utilized. Small increments of the peptide stock solution were injected into the buffer solution by means of a Hamilton syringe to obtain the desired concentrations. The surface pressure, $\pi = \gamma_0 - \gamma$, where γ_0 is the surface tension of the pure buffer and γ the surface tension of the peptide solution, was monitored by means of Whatman No. 1 filter paper connected to a Wilhelmy balance. Measurements were performed at ambient temperature (21 ± 1 °C).

For insertion experiments two compartments of the trough were used. The monolayer was formed by depositing a drop of lipid dissolved in hexane/ethanol (9:1, v/v) on the buffer surface between the two movable barriers and was then left to stabilize for about 15 min. The initial area, A (typically around 50 cm^2), contained n_L lipid molecules of area A_L.[2] Peptides were injected through the lipid monolayer into the buffer subphase and were left to equilibrate between the aqueous phase and the lipid phase for about 20 min. The surface pressure was kept constant during the insertion experiments by means of an electronic feedback system. The penetration of n_P peptide molecules of area A_P into the monolayer thus gave rise to an area expansion, ΔA. The mole fraction of peptide in the monolayer is defined as $X_b = n_P/n_L$, and can be evaluated from the relative area increase, $\Delta A/A$, provided A_L and A_P are known (cf. eq 1) (Seelig, 1987).

$$X_b = n_P/n_L = (\Delta A/A)(A_L/A_P) \quad (1)$$

As a first approximation the binding to the lipid membrane can be described in terms of a simple partition equilibrium:

$$X_b = K_{app}C_{eq} \quad (2)$$

For reasons explained below the partition constant must be

[2] The variation of the lipid area, A_L, is small in the pressure range under investigation.

considered as an "apparent" binding constant only.

In order to penetrate into a lipid monolayer with a lateral pressure π, a peptide molecule has to perform the work

$$\Delta W = \pi A_P \quad (3)$$

where the penetration area, A_P, is the area which the peptide occupies in the lipid monolayer. The free energy of penetration will therefore vary with the monolayer surface pressure. According to Boguslavsky et al. (1994) the variation of the binding constant with pressure is given by

$$K = K_0 \exp(-\pi A_P/kT) \quad (4)$$

Combining eqs 1 and 4 yields the surface pressure dependence of the relative area increase, $\Delta A/A$, at constant C_{eq}[2]:

$$\Delta A/A = (A_P/A_L)K_0 C_{eq} \exp(-\pi A_P/kT) \approx (\text{const})\exp(-\pi A_P/kT) \quad (5)$$

The measured pressure dependence of the $\Delta A/A$ curves can then be used to determine the area requirement of the peptide in the membrane, assuming a constant penetration area, A_P.

Evaluation of Binding Isotherms Taking into Account the Electrostatic Interactions. The electric surface charge density, σ, of a lipid layer is given by

$$\sigma = (e_0/A_L)[-X_{PG}(1 - X_{Na^+}) + z_b X_b]/[1 + (A_P/A_L)X_b] \quad (6)$$

where e_0 is the elementary charge, A_L the area per lipid molecule, and X_{PG} the mole fraction of negatively charged lipid. X_{Na^+} denotes the mole fraction of bound Na^+ per total POPG (Beschiaschvili & Seelig, 1990). X_b is the mole fraction of bound peptide of valence z_b per mole of *total* lipid. The term $(A_P/A_L)X_b$ corrects for the membrane expansion due to peptide penetration (Seelig, 1987). A membrane with an electric surface charge density, σ, gives rise to a surface potential, ψ_0. The quantitative relationship between the two parameters is provided by the Gouy−Chapman equation [cf. McLaughlin (1977, 1989)]:

$$\sigma^2 = 2000\epsilon_0\epsilon_r RT\sum_i C_{i,eq}(e^{-z_i F_0 \psi_0/RT} - 1) \quad (7)$$

where ϵ_0 is the permitivity of free space, ϵ_r the dielectric constant of water, $C_{i,eq}$ is the concentration of the ith electrolyte in the bulk aqueous phase (in moles per liter), F_0 the Faraday constant, RT the thermal energy, and z_i the signed valence of the ith species. Knowledge of the surface potential, Ψ_0, allows the calculation of the concentration, $C_{i,M}$, of a particular ion, i, at the interface according to the Boltzmann relation

$$C_{i,M} = C_{i,eq} \exp(-z_i F_0 \psi_0/RT) \quad (8)$$

The surface concentration, $C_{i,M}$, then determines the binding to the lipid membrane.

Using the interfacial concentration, C_M, of the peptide, instead of its bulk concentration, C_{eq}, the equilibrium between the plane of binding and the interfacial aqueous layer is described by a partition equilibrium of the form

$$X_b = K_p C_M \quad (9)$$

where K_p is the surface partition constant or "intrinsic binding" constant.

In the present analysis, the intrinsic binding constant K_p is the only free parameter whereas all other parameters can be deduced by independent measurements. (i) The amount of bound peptide per mole of lipid, X_b, was measured by monolayer expansion measurements and by high-sensitivity titration calorimetry. (ii) The effective charge of the peptide, z_b, was determined from a measurement of the pK values of the N-terminal amino groups and the charged peptide side chains (Seelig, 1990). For (Arg[9])SP and (Nle[9])SP the pK of the N-terminal amino group was 7.1. In (AcPro[2], Arg[9])-SP the N-terminal amino group is acylated. The pK values of Lys[3] and the guanidino groups of the Arg[1] and Arg[9] were >8.5 at the concentrations used for binding studies (S. Lotz & A. Seelig, unpublished results). These side chains are therefore fully protonated in the slightly acidic environment close to the negatively charged lipid membrane. The effective charge of the N-terminal amino group was then calculated from its pK and the pH value at the membrane surface [cf. Seelig et al. (1993)]. The effective charge, z_b, of the peptide is thus the sum of the charges of the side chains plus that of the amino terminal.

In the case of high-sensitivity titration calorimetry the measured heat of reaction, $\sum\Delta h_i$, is related to the amount of bound peptide according to (Beschiaschvili & Seelig, 1992):

$$\sum \Delta h_i = \Delta H X_i C_L^{\,o} V_{cell} \quad (10)$$

where ΔH is the molar heat of binding of the peptide, $C_L^{\,o}$ is the lipid concentration in the cell (only the outer layer of the lipid vesicles is considered, corresponding to 60% of the total lipid concentration), V_{cell} is the volume of the measuring cell, and X_i is the degree of binding after n_i injections.

Biological Assays. The binding experiments with ^{3}H-SP were performed using homogenates of bovine spinal cord exhibiting a high density of NK-1 receptors. For ^{3}H-neurokinin A (NKA) assays hamster urinary bladder homogenates with a high density of NK-2 receptors were used. The procedures are described elsewhere (Greiner, 1985). IC_{50} represents the concentration of unlabeled ligand that causes 50% inhibition of specifically bound radiolabeled ligand.

In vitro activity measurements were performed on the rabbit jugular vein (Nantel et al., 1990). This essay is selective for the NK-1 receptor. EC_{50} represents the concentration of the peptide which leads to half-maximal response in the essay.

RESULTS

Peptide Conformations Induced by SDS Micelles and Small Unilamellar Lipid Vesicles. Figure 1 displays CD spectra of (Arg[9])SP, (AcPro[2], Arg[9])SP, and (Nle[9])SP in solution, in the presence of SDS micelles, and with uncharged and charged lipid vesicles, respectively. CD spectra of SP under the same experimental conditions are also included. In buffer (spectrum 1, Figure 1A−D) the four peptides exhibit identical spectra with minima around 200 nm, typical for a predominantly random coil conformation. The minima are, however, less pronounced than expected from reference spectra due to the positive absorption band of phenylalanine around 200 nm (Holladay et al., 1977; Brahms & Brahms, 1980).

Addition of SDS micelles (spectrum 4, Figure 1A−D) gives rise to α-helix-like spectra for all four peptides. Changing the peptide-to-SDS ratio from 2 mmol/mol (Figure 1) to 80 mmol/mol (data not shown) does not influence the spectra. It can therefore be concluded that under the conditions used in Figure 1 the peptides are completely bound to the SDS micelles. The intensity ratio of the minima at

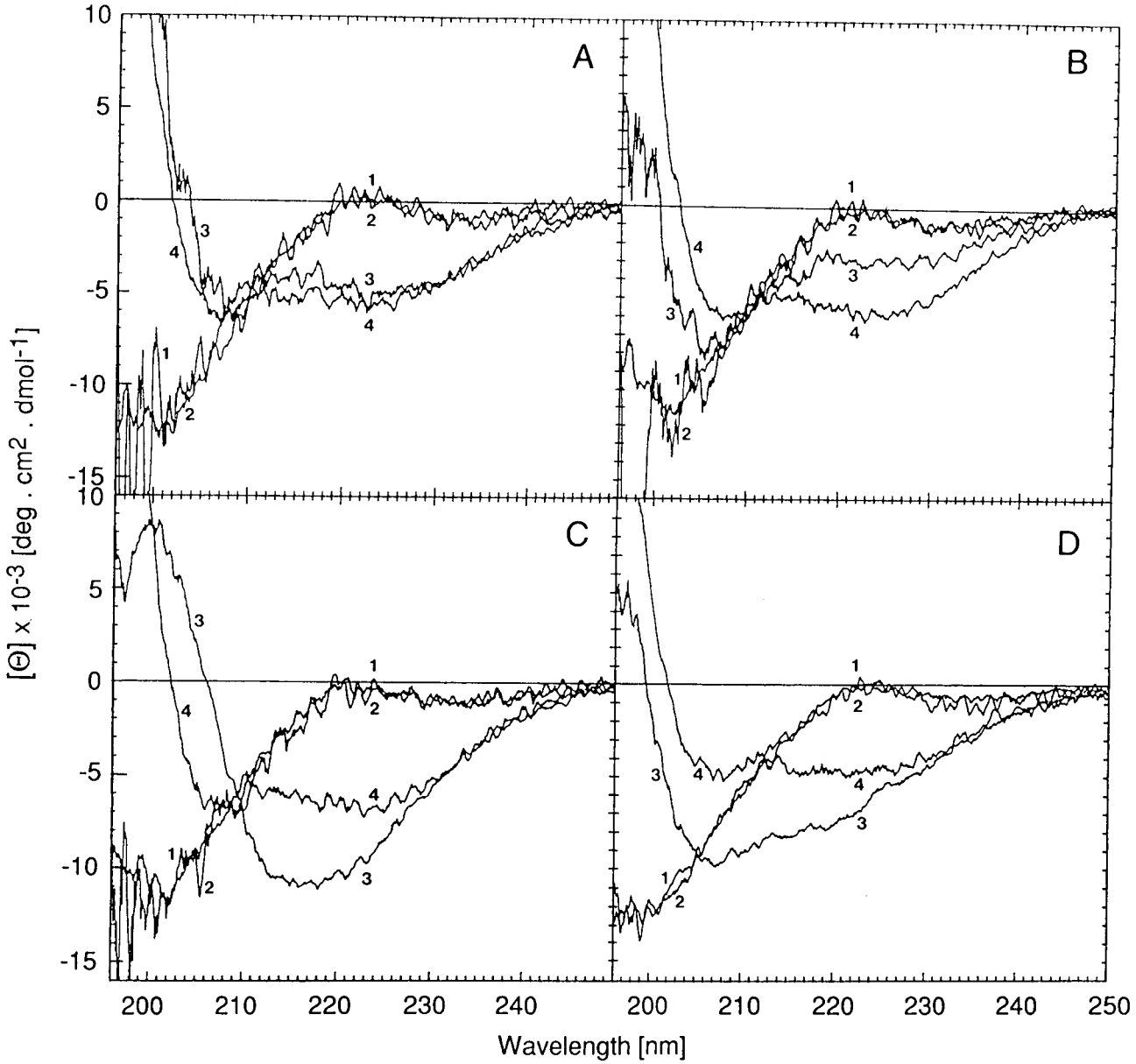

FIGURE 1: CD spectra of (Arg ^{9})SP (A), (AcPro^{2}, Arg^{9})SP (B), (Nle^{9})SP (C), and SP (D) in 10 mM Tris-HCl buffer (pH 7.4, 154 mM NaF) (1) and in the presence of POPC (2), POPG vesicles (2 mM) (3), and SDS micelles (30 mM) (4). Peptide concentrations for all measurements were close to 6×10^{-5}M.

208 nm and 222 nm is $R \approx 1$ for all four peptides. The residue ellipticities differ, however, and are 4500 deg cm^2 dmol^{-1} for SP [in agreement with Rolka et al. (1986) and Williams and Weaver (1990)], 6000 deg cm^2 dmol^{-1} for (Arg^9)SP and (AcPro^2, Arg^9)SP, and 7000 deg cm^2 dmol^{-1} for (Nle^9)SP. The degree of α-helicity was estimated using the equation of Chen et al. (1974) assuming that the absorption at 222 nm is exclusively due to an α-helix:

$$\Theta_H^n = (1 - k/n)\Theta_H^\infty \qquad (11)$$

Here Θ_H^n and Θ_H^∞ are the mean residue ellipticities of an α-helix of n residues and of an infinitely long helix, respectively, and $k = 2.57$ is a wavelength-dependent constant. Θ_H^n at 222 nm was thus calculated to be −30 300 deg cm^2 dmol^{-1} for SP, (Arg^9)SP and (Nle^9)SP, and as −29 300 deg cm^2 dmol^{-1} for (AcPro^2, Arg^9)SP, assuming $\Theta_H^\infty = -39\,500$ deg cm^2 dmol^{-1} (Chen et al., 1974).

A complication in evaluating the helix content of SP and its analogues arises from the additional contributions of the aromatic amino acids, a problem which has been neglected in previous analyses. The average contribution of a single phenylalanine residue was taken into account as 17 500 deg cm^2 dmol^{-1} molar ellipticity at 222 nm (Holladay & Puett, 1976; Holladay et al., 1977). With this correction, the helix contents were calculated as 30% (3.3 residues) for (Arg^9)-SP, 32% (3.6 residues) for (AcPro^2, Arg^9)SP, 34% (3.7 residues) for (Nle^9)SP, and 25% (2.8 residues) for SP (Table 1). For comparison, the helix content of (Sar^9, Met(O$_2$)^{11})-SP, which is the most specific synthetic NK-1 agonist known to date, is only 20% (2.2 residues) and is also included in Table 1.[3]

Addition of neutral POPC vesicles has no influence on the CD spectra (spectrum 2, Figure 1A−D), providing a first indication that the peptides under investigation cannot penetrate into a neutral POPC bilayer.

A different situation is encountered if the membrane carries a negative surface charge. In the presence of POPG vesicles

[3] The helix content was evaluated by the method outlined above using previously published CD spectra of (Sar^9, Met(O$_2$)^{11})SP (Seelig, 1992).

Table 1: Comparison of Physical-Chemical and Biological Parameters for SP and Its Agonists

compound	z	% α-helix in SDS micelles	K_p (M^{-1})	K_{app} (M^{-1}) 100% PG	IC_{50} (nM) ^{3}HSP[a]	IC_{50} (nM) ^{3}HNKA[b]	EC_{50} (nM) RJV[c]
SP	3	25	9 ± 1	$\sim 1 \times 10^4$	2	200	4
(Sar^9, $Met(O_2)^{11}$)SP	3	20	<1	nd	10	nd	nd[d]
(Arg^9)SP	4	30	10 ± 1	$\sim 1 \times 10^5$	200	>10 000	40
($AcPro^2$,Arg^9)SP	2	32	9 ± 1	$\sim 1 \times 10^3$	3 000	3 000	27
(Nle^9)SP	3	34	39 ± 3	$\sim 2 \times 10^4$	90	>10 000	3.4

[a] Measured in bovine dorsal horn homogenates. [b] Measured in hamster urinary bladder homogenates. [c] Measured on rabbit jugular vein. [d] EC_{50} of (Sar^9, $Met(O_2)^{11}$)SP was not determined in this work (nd), but was shown previously to be practically identical to that of SP (Nantel et al., 1990).

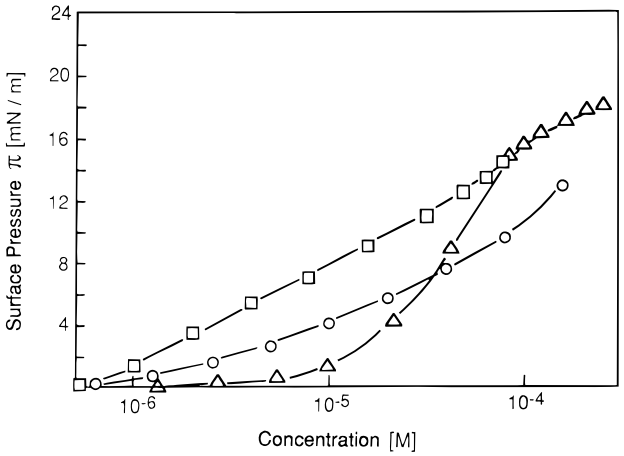

FIGURE 2: Surface pressure, π, as a function of the concentration of (Arg^9)SP (△), ($AcPro^2$, Arg^9)SP (○) and (Nle^9)SP (□) measured in 10 mM Tris-HCl buffer (pH 7.4, 154 mM NaCl).

(peptide-to-lipid ratio = 30 mmol/mol) all four peptides undergo conformational changes which are, however, not identical (cf. spectrum 3, Figure 1A−D). (Arg^9)SP exhibits an α-helix-like double minimum at 208 and 222 nm with an intensity ratio of $R \approx 1$, indicating practically the same degree of helicity as in SDS micelles. In contrast, (Nle^9)SP exhibits a spectrum with a broad minimum at 217 nm. This spectrum is typical for peptides in the β-sheet conformation. It can be explained by the high concentration of the cationic peptide at the surface of the negatively charged POPG vesicles, leading to aggregation and formation of β-sheet structures. At *low* concentrations of (Nle^9)SP (peptide-to-lipid ratio < 7 mmol/mol), β-sheet structure formation is much less pronounced and the CD-spectrum is helix-like (data not shown). The CD spectra of ($AcPro^2$, Arg^9)SP and SP are more complex. ($AcPro^2$, Arg^9)SP also adopts a partially helical conformation, but the CD-spectrum has a lower ellipticity ratio of $R \approx 0.37$, indicating a decrease in helicity and a concomitant increase in random coil conformation. Finally, the spectrum of SP itself is intermediate between those of ($AcPro^2$, Arg^9)SP and (Nle^9)SP.

Gibbs Adsorption Isotherms and Peptide Surface Areas. Gibbs adsorption isotherms for the three SP analogues are shown in Figure 2. The experimentally observed surface pressure is plotted against the logarithm of the peptide concentration. At low concentrations ($c_{eq} < 3 \times 10^{-5}$ M) the surface activities of the peptides increase in the order (Arg^9)SP < ($AcPro^2$, Arg^9)SP < (Nle^9)SP. The least surface active compound is (Arg^9)SP, carrying four positively charged groups, and the most surface active compound is (Nle^9)SP with an uncharged, hydrophobic amino acid in position 9 of the amino acid sequence. The intermediate surface activity of ($AcPro^2$, Arg^9)SP is very similar to that of the parent compound SP (Seelig, 1990). At high peptide concentrations the order of the surface activities changes. This can be explained by a deprotonation of (Arg^9)SP at residue 9 (S. Lotz and A. Seelig, unpublished results) leading to the same surface activity as that of (Nle^9)SP. From the slopes of the linear parts of the Gibbs adsorption isotherms the excess concentration, Γ, of the solute at the air−water interface can be determined as

$$\Gamma = (1/RT)(\delta\pi/\delta \ln c) \quad (12)$$

where RT is the thermal energy. Γ allows the evaluation of the surface area, A_S, of an individual peptide molecule at the air−water interface according to

$$A_S = 1/(\Gamma N_A) \quad (13)$$

where N_A is the Avogadro number.

At high concentrations ($c > 10^{-4}$ M) the three peptides exhibit very similar surface areas in the range of 145 ± 5 Å^2, which is comparable to the surface area of SP if also measured at high peptide concentrations (Seelig, 1990). At low concentrations (1.5×10^{-6} to 1×10^{-5} M), the surface area of ($AcPro^2$, Arg^9)SP is 240 ± 5 Å^2, which is again identical to that of SP in the same concentration range (Seelig, 1990). The surface area of (Arg^9)SP is also 240 ± 10 Å^2 for $c \approx 5 \times 10^{-6}$ to 1×10^{-5} M but is somewhat larger at lower concentrations, most probably due to the stronger electrostatic repulsion. The β-sheet-forming peptide (Nle^9)SP adopts a small surface area of 145 ± 5 Å^2 already at low concentrations ($c > 10^{-6}$ M).

Peptide Penetration as a Function of the Monolayer Surface Pressure. The relative area increase, $\Delta A/A$, of lipid monolayers upon peptide penetration was measured as a function of the lateral pressure, π. Monolayers were composed of either neutral POPC or negatively charged POPG or mixtures of the two. As an example, Figure 3 displays the penetration of (Arg^9)SP into the three types of monolayers. A semilogarithmic plot of the area change versus the surface pressure yields straight lines (not shown). From their slopes the penetration areas, A_P, of the peptides were derived according to eq 5. The solid lines in Figure 3 were calculated with these areas. Figure 4 then summarizes the penetration areas, A_P, as derived from Figure 3 and analogous mesurements. The A_P values were found to depend on the peptide involved as well as on the lipid composition of the monolayer.

An approximately linear decrease of A_P with increasing negative surface charge density of the monolayer was observed for SP, ($AcPro^2$, Arg^9)SP, and (Arg^9)SP. For (Nle^9)SP only two A_P values were measured, and the linearity is thus not fully proven.

Binding Isotherms Measured by Means of the Monolayer Expansion Method. Monolayers at a surface pressure of 32 mN/m (Seelig, 1987) were used as model systems for planar

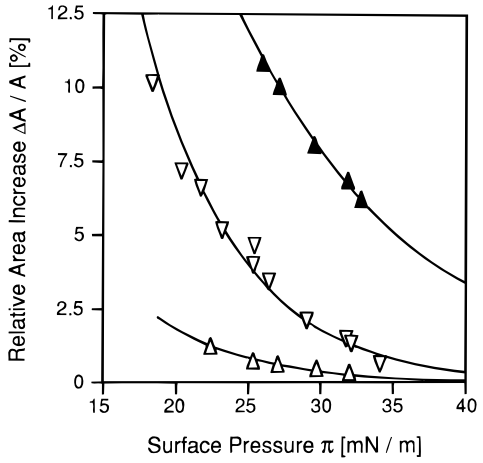

FIGURE 3: The relative area increase, $\Delta A/A$, due to the insertion of (Arg^9)SP into POPC (△), POPC/POPG (75/25 mol/mol) (▽), and POPG (▲) monolayers, respectively, as a function of the monolayer surface pressure, π. The peptide concentrations were 5.3×10^{-6} M (△), 6.6×10^{-6} M (▽), and 6.6×10^{-7} M (▲). Measurements were performed at pH 7.4 (10 mM Tris-HCl, 154 mM NaCl).

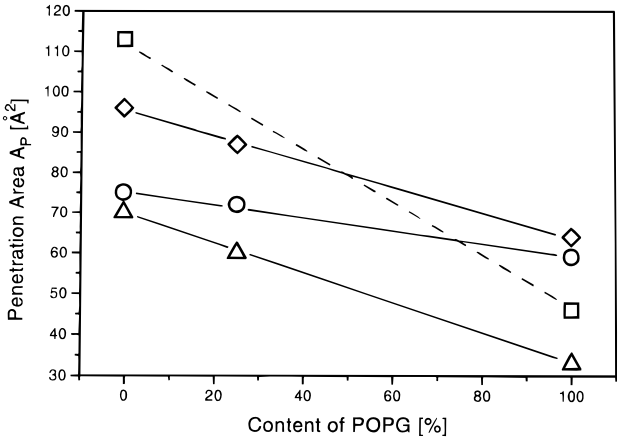

FIGURE 4: Insertion areas, A_P of (Arg^9)SP (△), (AcPro^2, Arg^9)SP (○), SP (◇), and (Nle^9) (□) as a function of the POPG content in POPC/POPG monolayers. The diameter of the symbols corresponds approximately to the error in A_P.

lipid bilayers. The relative area increase, $\Delta A/A$, of lipid monolayers, composed of either POPC/POPG (75/25 mol/mol) or pure POPG, due to the insertion of increasing amounts of (Arg^9)SP, (AcPro^2, Arg^9)SP, and (Nle^9)SP, was measured as a function of the peptide bulk concentration. Since the amount of bound peptide was smaller than 1% of the total peptide concentration, the equilibrium concentration, C_{eq}, was assumed to be equal to the total peptide concentration, C_{tot}. From the relative area increase, $\Delta A/A$, the mole fraction of bound peptide, X_b, was determined according to eq 1. The area expansion curves were transformed into binding isotherms using a lipid area, $A_L = 65$ Å^2, for POPC and POPG (Evans et al., 1987; Taschner, 1992) and the peptide penetration areas, A_P, summarized in Figure 4. The binding isotherms of (Arg^9)SP, (Nle^9)SP, and SP with POPC/POPG (75/25 mol/mol) monolayers and of (AcPro^2, Arg^9)-SP with POPG monolayers are shown in Figure 5. The solid lines represent the theoretical binding isotherms calculated by means of the Gouy−Chapman theory (Seelig et al., 1993).

Peptide Binding Measured by High-Sensitivity Titration Calorimetry. The binding of (Arg^9)SP to lipid membranes was also investigated with high-sensitivity titration calorimetry. Small increments (10 μL) of an (Arg^9)SP solution (5.23×10^{-4} M) were injected into the calorimeter cell containing a large excess of a lipid vesicle suspension (11.19 mg of lipid/mL). The sonified lipid vesicles (diameter ≈ 30 nm) were composed of POPC/POPG (75/25 mol/mol). Each injection gave rise to approximately the same heat of reaction since the peptide was immediately bound to the negatively charged lipid vesicles. The binding enthalpy, ΔH, of the reaction was −5.3 kcal mol^{-1}. Injecting the same peptide into buffer solution without lipids led to only a small heat of dilution (+0.2 kcal/mol), which was taken into account in the calculation of the binding enthalpy.

The reverse experiment, i.e., the titration of lipid vesicles into a peptide solution, allowed the determination of the binding isotherm. The calorimeter cell ($V_{cell} = 1.278$ mL) contained a 44.8 μM (Arg^9)SP solution in buffer. Due to the lower sensitivity of this method, peptide concentrations are about 1 order of magnitude higher than in the monolayer measurements. Each peak in the titration experiment shown in Figure 6A corresponds to the injection of 10 μL of sonified POPC/POPG (75/25 mol/mol) vesicles. The lipid concentration was 26.6 mM, but only the outer surface of the lipid vesicles (60% of the total lipid) is accessible to peptide molecules. The heat of reaction decreases with consecutive injections since less and less peptide is available for binding. Figure 6B shows the cumulative heat of reaction as a function of the number of injections, which, in turn, can be used to calculate the binding isotherm as described above (Figure 5).

Biological Assays. The competitive binding of the SP analogues to NK-1 receptors in bovine dorsal horn homogenates and to NK-2 receptors in homogenates of the hamster urinary bladder was measured in the presence of ^{3}H-SP and ^{3}H-NKA, respectively, as described previously (Greiner, 1985). The resulting inhibitory constants, IC_{50}, are summarized in Table 1. The IC_{50} values for the binding to the NK-1 receptor increase in the order SP < (Sar^9, Met(O$_2$)^{11})-SP < (Nle^9)SP < (Arg^9)SP < (AcPro^2, Arg^9)SP. The substitution of Gly^9 (no side chain) by Nle (57-Da side chain) or Arg (100-Da side chain) shows that the NK-1 receptor tolerates a large side chain increase in this position without a complete loss of activity. The IC_{50} values decrease, however, in parallel to the side chain increase. On the other hand, the additional C-terminal charge of Arg^9 compared to Nle^9 does not further reduce the binding affinity to the receptor. It is interesting to note that the loss of the Arg^1 in (AcPro^2, Arg^9)SP leads to a loss of the specificity for the NK-1 receptor.

The EC_{50} values seem to be more sensitive to the C-terminal charge than the IC_{50} values, as seen in Table 1. Whereas (Nle^9)SP has essentially the same agonist activity as SP, the agonist activity of (Arg^9)SP is approximately 10 times lower.

DISCUSSION

In the present study we have used a physical-chemical approach to provide insight into the conformation of SP and synthetic SP-agonists in different environments and to map the conformational space available to these ligands. In addition, we have provided quantitative data on the size requirement of the peptides in the lipid membrane and on their electrostatic and hydrophobic lipid binding affinities. Since the receptor binding site comprises extracellular as well as transmembrane segments, some of its properties are

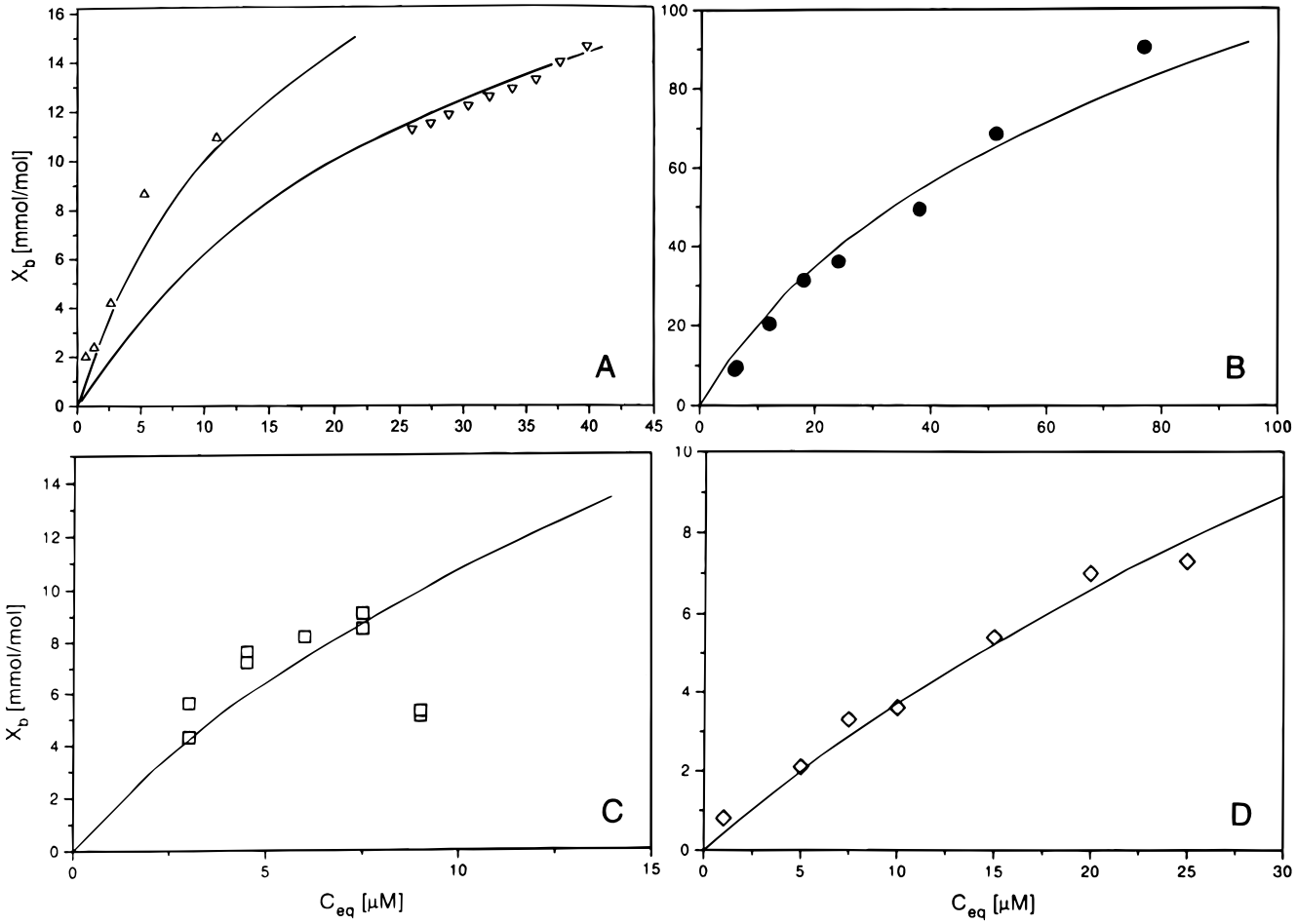

FIGURE 5: Binding of (Arg^9)SP (A, △), (Nle^9)SP (C, □), and SP (D, ◇), to POPC/POPG (75/25 mol/mol) monolayers and of (AcPro^2, Arg^9)SP (B, ●) to POPG monolayers as measured by means the monolayer expansion method at pH 7.4 (10 mM Tris-HCl, 154 mM NaCl). Monolayers were kept at a constant surface pressure, $\pi = 32$ mN/m at 21 ± 1 °C. Binding of (Arg^9)SP (A, ▽) to small unilamellar POPC/POPG (75/25 mol/mol) vesicles as measured by high-sensitivity titration calorimetry at 28 °C. The solid lines correspond to the best theoretical fit to the data and are calculated with the following intrinsic binding constants: $K_p = 10$ M^{-1} for (Arg^9)SP (△), and $K_p = 5.2$ M^{-1} for (Arg^9)SP (▽), $K_p = 9$ M^{-1} for (AcPro^2, Arg^9)SP (●), $K_p = 39$ M^{-1} for (Nle^9)SP (□), and $K_p = 9$ M^{-1} for SP (◇).

probably modeled by the amphiphilic lipid−water interface. Thus, even though a membrane-mediated receptor mechanism can be excluded under biologically relevant conditions (for reasons that will be discussed in the following), the interfacial conformations deduced in the presence of artificial interfaces probably resemble the bound conformation at the receptor.

Peptide Conformations in the Presence of SDS Micelles and Lipid Vesicles. In the presence of negatively charged SDS micelles, SP and its agonists show helix-like CD spectra. The spectra suggest short, helix-like segments consisting of about ∼4 amino acid residues for the newly synthesized SP-agonists, ∼3 for SP, and ∼2 for (Sar^9, Met(O$_2$)^{11})SP. The substitution of Gly^9 in SP by Nle or Arg, which both exhibit a higher helical propensity than Gly, thus *increases* the length of the helical segment by about 1 residue whereas the substitution by the structure breaking Sar *reduces* it. This observation suggests that the α-helical segment can be assigned to residues 7−10 for (Nle^9)SP and (Arg^9)SP, 7−9 for SP, and 7−8 for (AcPro^2, Arg^9)SP. This conclusion is further corroborated by a comparison of SP with the related neuropeptide eledosin (Wilson et al., 1994). Eledosin has a primary sequence closely related to that of SP. Its CD spectrum in the presence of SDS micelles reveals the same degree of helicity as determined for SP. NMR measurements identify the helical region to be composed of residues 6−10 with dynamic fraying at both ends of the peptide. The highest degree of order for eledosin was observed for residues 7−9, the same residues which have been deduced above from substitution experiments for SP. In the presence of SDS micelles the two peptides thus might adopt a similar conformation.

No secondary structure formation is observed for SP and its analogues in the presence of neutral POPC bilayers. An explanation is provided by the monolayer experiments. An area expansion, indicating a peptide insertion into the monolayer, is only detected at low packing densities of the POPC monolayer. However, at surface pressures >32 mN/m peptide insertion comes to a complete halt. From different types of physical-chemical experiments it is well established that a monolayer packing density of 32 ± 1 mN/m is equivalent to the molecular packing in a planar POPC bilayer (Demel et al., 1975; Blume, 1979; Seelig, 1987). Hence it can be concluded that the affinity of SP and its analogues to electrically neutral lipids is too low to cause any detectable penetration into the POPC bilayer.

In the presence of POPG vesicles secondary structure formation is more complex. (Arg^9)SP and (AcPro^2, Arg^9)-SP, which both exhibit a C-terminal charge, show helix-like structures, while (Nle^9)SP and SP undergo a concentration dependent conformational change. At low peptide-to-lipid ratios (<7 mmol/mol) the helix-like conformation is pre-

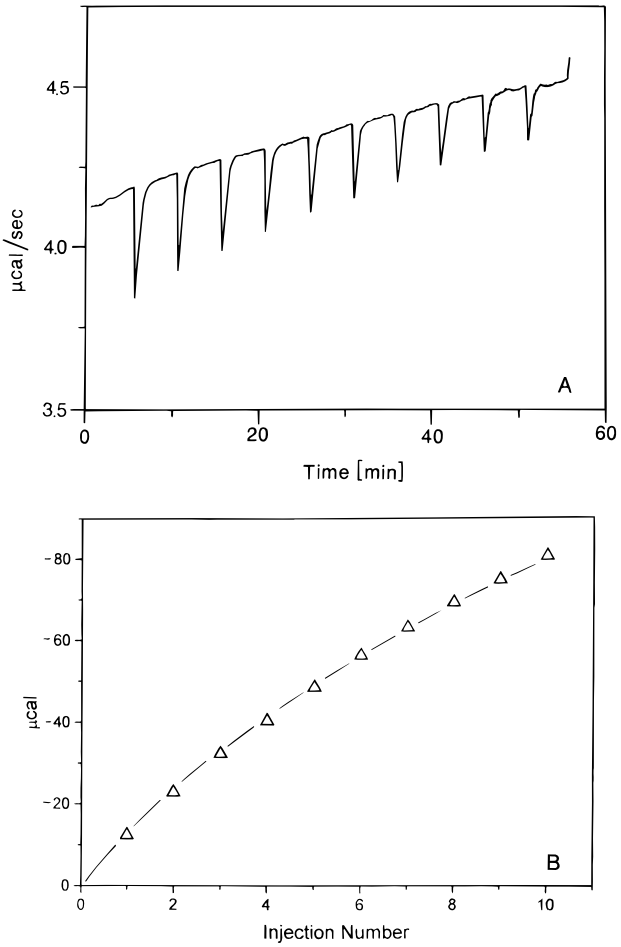

FIGURE 6: Titration calorimetry of an (Arg^9)SP solution (4.48×10^{-4} M) with small unilamellar POPC/POPG (75/25 mol/mol) vesicles (26.6 mg/mL) at pH 7.4 (50 mM phosphate buffer, 114 mM NaCl) at 28 °C. The volume of injection was 10 μL. (A) Calorimeter tracing. (B) Cumulative reaction enthalpy as a function of the number of injections.

dominant for both peptides. At a peptide-to-lipid ratio of 30 mmol/mol (Figure 1) a β-sheet contribution is predominant for (Nle^9)SP while it is still small for SP. A predominant β-sheet structure for SP is only observed at a much higher peptide-to-lipid ratio as shown previously (Shibata et al., 1985). A similar lipid-induced β-sheet formation has been reported for Alzheimer peptides (Terzi et al., 1994, 1995).

Peptide Dimensions. At low peptide concentration the surface areas, A_S, of SP, (Arg^9)SP, and ($AcPro^2$, Arg^9)SP are almost identical and amount to about 240 ± 10 Å^2. The more hydrophobic (Nle^9)SP has a smaller surface area with $A_S = 145 \pm 5$ Å^2. For a molecular interpretation of the measured surface areas the dimensions of the peptides in either an α-helical or a β-sheet conformation were estimated by molecular modeling. The cross-sectional areas, measured parallel and perpendicular to the helix axis, are denoted $A_{\alpha||}$ and $A_{\alpha\perp}$, respectively. Taking into account fraying at both ends of the helix the calculation yields $A_{\alpha||} = 250 \pm 10$ Å^2 and $A_{\alpha\perp} = 165 \pm 8$ Å^2 for (Arg^9)SP and $A_{\alpha||} = 237 \pm 10$ Å^2 and $A_{\alpha\perp} = 163 \pm 8$ Å^2 for (Nle^9)SP. The cross-sectional areas of the same two peptides modeled in a β-sheet structure oriented perpendicularly to the membrane surface are $A_{\beta\perp} = 85 \pm 5$ Å^2. The experimentally determined surface area, $A_S = 240 \pm 10$ Å^2 of SP, (Arg^9)SP, and ($AcPro^2$,Arg^9)SP agrees with $A_{\alpha||}$. This result suggests that the three peptides adopt a partially helical conformation at the air−water interface and are oriented with their long axes parallel to the surface.

The air−water interface mimics the lipid−water interface since a region of low dielectric constant (air, $\epsilon \approx 1$; hydrocarbon, $\epsilon \approx 2$) is in contact with a region of high dielectric constant (water, $\epsilon \approx 78$). The orientation at the air−water interface thus provides a first clue for the possible alignment of the peptides at the membrane surface.

A surface area of $A_S = 145 \pm 5$ Å^2 is found for (Nle^9)SP (for concentrations $c_{eq} > 1$ μM) and also for SP, (Arg^9)SP, and ($AcPro^2$, Arg^9)SP at *high* peptide concentrations. This surface area is even smaller than the theoretical cross-sectional area of $A_{\alpha\perp}$ but is consistent with a β-sheet structure. Nle is a well-known β-sheet structure promoter (Arfmann et al., 1977), and the CD spectra of (Nle^9)SP in the presence of POPG vesicles are compatible with β-sheet structure formation. Charge repulsion effects which are stronger in the closely packed β-sheet structure than in the helical arrangement and/or an initial bend in the charged N-terminal sequence might be responsible for the relatively large surface area such that $A_S > A_{\beta\perp}$.

Peptide Penetration into the Membrane Surface. A more detailed insight into the peptide−lipid interaction is provided by the peptide penetration area, A_P, derived from the pressure dependence of the monolayer binding isotherms. The penetration area, A_P, is a relatively recent concept (Boguslavsky et al., 1994), and the present study is a first systematic application to small peptides. The A_P values of the neuropeptides fall in the range 33 Å^2 < A_P < 113 Å^2 and are thus distinctly smaller than the surface areas, A_S, and the theoretical cross-sectional areas, $A_{\alpha||}$, $A_{\alpha\perp}$, and $A_{\beta\perp}$. A complete insertion of these peptides as α-helices, with their long molecular axes perpendicular to the lipid surface (Schwyzer et al., 1986), can therefore be excluded for SP and its agonists. The relatively small penetration areas rather suggest that the peptides insert only partially into the lipid membrane, most probably with the hydrophobic residues 7−9 or 10 forming the helical loop or turn. Geometric constraints would then dictate a primarily parallel orientation of the long molecular axis with respect to the membrane surface. This molecular picture is in agreement with a previous interpretation of NMR measurements for SP (Duplaa et al., 1994).

Figure 4 further demonstrates that the penetration areas, A_P, depend on the nature of the peptide as well as on the surface charge density of the monolayer. For electrically neutral monolayers the penetrating peptide portion, A_P, is largest for the most hydrophobic peptide (Nle^9)SP and decreases with increasing hydrophilicity in the order (Nle^9)-SP > SP > ($AcPro^2$, Arg^9)SP > (Arg^9)SP. Furthermore, the insertion areas, A_P, decrease linearly with increasing POPG content of the monolayer. The decrease of the area, A_P, is proportional to the peptide charge and follows the order ($AcPro^2$, Arg^9)SP < SP < (Arg^9)SP. For (Nle^9)SP which has the same charge as SP, the relative area change is, however, more pronounced than for the other peptides. This is most likely due to a transition from a partially helix-like conformation to a β-sheet conformation as the negative surface charge density of the monolayer increases, while the other three peptides remain in a partially helical conformation even with negatively charged membranes (cf. Figure 1).

Thermodynamic Analysis of Binding Isotherms. Electrostatic and Hydrophobic Interactions. Binding isotherms were derived from monolayer expansion measurements and,

in part, from high-sensitivity titration calorimetry. Close agreement was obtained for the two methods when applied to comparable systems (peptide binding to monolayers at 32 mN/m surface pressure).

The conventional Scatchard analysis of the binding isotherms led to nonlinear Scatchard plots (not shown), indicating a more complex binding behavior than anticipated on the basis of a Langmuir adsorption model [cf. Seelig and Macdonald (1989)]. Nevertheless, from the initial part of the binding isotherms apparent binding constants, K_{app}, could be determined. The K_{app} values are listed in Table 1 and fall in the range of 10^3-10^5 M^{-1} for pure POPG monolayer membranes. Inspection of Table 1 demonstrates that (i), for a given peptide the binding constant, K_{app} increases with the negative surface charge density of the lipid monolayer and that (ii), for a constant lipid composition, K_{app} increases with the charge of the peptide. Together, these results provide evidence for a distinct electrostatic contribution to the binding process.

A physically more meaningful type of analysis is therefore to separate electrostatic attraction from hydrophobic penetration. As mentioned above, the negative membrane charge leads to an accumulation of cationic peptides at the membrane surface. The surface concentration, C_M, is thus distinctly larger than the bulk concentration, C_{eq}. We have hence calculated C_M from the experimental data by means of the Gouy−Chapmann theory (cf. Materials and Methods). C_M, in turn, was inserted into eq 9 to yield the intrinsic binding constant K_p with $K_p = 10 \pm 1$ M^{-1} for (Arg^9)SP, $K_p = 9 \pm 1$ M^{-1} for (AcPro^2, Arg^9)SP and SP, and $K_p = 39 \pm 3$ M^{-1} for (Nle^9)SP.[4]

The intrinsic binding constants, K_p, are 2−3 orders of magnitude smaller than the apparent binding constants, K_{app}. This can be traced back to the much higher concentration C_M compared to C_{eq}, which shows that K_{app} is mainly determined by electrostatic interactions. More importantly, the intrinsic binding constant remains constant over the whole concentration range measured, whereas K_{app} is valid only for the initial phase of the binding isotherm. The intrinsic binding constants represent the hydrophobic contribution to the peptide−membrane equilibrium. Indeed, (Nle^9)SP which is the most hydrophobic of the four peptides also has the largest binding constant K_p.

The binding constant, K_p, can be converted into the free energy of binding, ΔG, according to[5]

$$\Delta G = -RT \ln(55.5K_p) \qquad (12)$$

resulting in $\Delta G = -3.7$ kcal/mol for (Arg^9)SP, −3.6 kcal/mol for (AcPro^2, Arg^9), and −4.4 kcal/mol for the more hydrophobic (Nle^9)SP. The free energy contribution of a hydrophobic side chain with a hydrophobic template was estimated as −0.6 kcal/mol by Ptitsyn and Finkelstein (1983). Assuming that the binding of (Arg^9)SP ((Nle^9)SP) to the lipid membrane is caused by an insertion of the hydrophobic side chains of Phe^7, Phe^8, Leu^{10}, and Met^{11} (Phe^7, Phe^8, Nle^9, Leu^{10}, and Met^{11}), a free energy of −2.4 kcal/mol (-3.0 kcal/mol) is calculated, which is in broad agreement with the measurements. The thermodynamic analysis shows that the hydrophobic binding is primarily due to an interaction of the hydrophobic side chains and provides independent evidence that only a small portion of the peptide molecules inserts into the lipid membrane.

Is Lipid Binding Relevant for Receptor Binding? SP and the newly synthesized SP agonists are well soluble in buffer. The monolayer expansion studies and the thermodynamic titration experiments demonstrate that the neuropeptides do not bind to neutral POPC bilayers or POPC monolayers (at $\pi > 32$ mN/m). Penetration into the lipid membrane can only be achieved if the membrane carries a negative surface charge, thereby increasing dramatically the interfacial concentration of the cationic peptides. Postsynaptic membranes which harbor the NK-1 receptor most probably exhibit a similar transbilayer asymmetry as synaptic vesicles, with the extracellular side of the membrane containing only a small fraction of negatively charged lipids (Michaelson et al., 1983). In addition, the postsynaptic membrane has a high cholesterol content of 40% which, in turn, causes a tight packing of the membrane. This leads to an increase in the bilayer−monolayer equivalence pressure to 35 mN/m (Taschner, 1992). Since electrostatic attraction is weak and membrane penetration hindered via cholesterol, an appreciable membrane binding of SP, (Sar^9, Met(O$_2$)^{11})SP, and the three agonists can be excluded under physiological conditions. By the same reasoning, the formation of β-sheet structures as suggested by Choo et al. (1994) can also be excluded under physiological conditions. β-Sheet formation requires an increased concentration of the neuropeptides, which is only achieved with negatively charged membranes. With neutral membranes the interfacial concentration of SP and its derivatives will remain too low.

The intrinsic lipid binding constants as summarized in Table 1 reveal a low affinity of all neuropeptides for the membrane phase. A comparison of lipid binding with the respective IC_{50} values shows that neither an increase in the hydrophobic binding constant, as observed for (Nle^9)SP, nor an increase in the electrostatic binding constant, as noted for (Arg^9)SP, improves the binding to the receptor (Table 1). Indeed, an inverse relationship between lipid-binding and receptor-binding of SP agonists seems to exist, i.e., a high lipid affinity is associated with a low receptor affinity and vice versa. A similar behavior was also observed for somatostatin agonists (Seelig et al., 1993). The low penetration of agonists into the hydrophobic membrane interior suggests that the binding site at the receptor is extramembraneous, exhibiting an amphiphilic character. This is indeed supported by mutagenesis and heterologous expression experiments which have shown that several residues in the first and second extracellular segments of the NK-1 receptor are required for the high-affinity binding of SP and related agonists (Fong et al., 1992). In summary, it can be concluded that the probability of a lipid-mediated receptor binding of SP and its agonists is extremely low.

Structure−Activity Relationship. The binding affinity to the NK-1 receptor decreases in the order SP ∼ (Sar^9, Met(O$_2$)^{11})SP > (Nle^9)SP > (Arg^9)SP > (AcPro^2, Arg^9)SP. By correlating the structural knowledge derived for SP and its agonists with their functional activity, the conformation of SP in the bound state can be approximated. The common structural denominator of the "message segment" of SP,

[4] The binding constant deduced for SP is somewhat larger than that determined previously (Seelig & Macdonald, 1989) mainly for two reasons. First, the binding of Na^+ was included in the present Gouy−Chapman analysis [cf. Beschiaschvili and Seelig (1990)]. Secondly, the penetration area, A_P, instead of the larger surface area, A_S, was used for the evaluation in order to account for the only partial insertion of the peptide into the lipid membrane.

[5] The factor 55.5 corrects for the cratic contribution [cf. Cantor and Schimmel (1980)].

(Sar^9, Met(O$_2$)^{11})SP, and the newly synthesized agonists is a helix-like conformation for residues Phe^{7,8}. The function of this conformation is most probably to provide a hydrophilic face containing residues Gln^6 and Gly^9 and a hydrophobic face containing Phe^{7,8} and Leu^{10}, leading to an optimal positioning at the receptor binding site [cf. Cornell et al. (1989)]. The high sensitivity of Phe^7 to spatial modifications (Boyd et al., 1991) suggests a tight fit at the hydrophobic face. On the other hand, the present findings demonstrate that the hydrophilic face tolerates major enlargements at Gly^9 and even an additional charge. The replacement of Phe^7 by D-Trp as, e.g., in Spantide, eliminates the helix-like turn (Seelig & Dölz, 1991), reduces the conformational freedom of the message segment, and leads to a decrease of the binding affinity and to a loss of the agonistic activity at the NK-1 receptor (Folkers et al., 1984). Likewise, the present substitutions of Gly^9 by Nle or Arg also reduce the flexibility, this time by stabilizing the helical segment by approximately one residue. Again a decreases of the binding affinity for the receptor is observed. This result suggests that the formation of a stable helical "message" segment is, in fact, unfavorable for receptor binding. The IC$_{50}$ values for NK-1 binding are more influenced by the elongation of the side chain in position 9 than by the introduction of the cationic guanidino group, which again points to a rather hydrophilic environment of the binding site. This is further supported by the high affinity of (Sar^9, Met(O$_2$)^{11})SP which exhibits a distinctly more hydrophilic C-terminus than SP, due to the oxidation of Met^{11} (Seelig, 1992).

In contrast to receptor binding, *activity* seems to be more sensitive to the additional charge in position 9. This suggests that in order to trigger activity, the C-terminus has to reach a more hydrophobic environment and is consistent with an interaction of the agonist with the second transmembrane segment (Huang et al., 1994). The higher activity of SP and (Nle^9)SP could suggest that the formation of a β-sheet-like structure connecting two different receptor sequences might be necessary in order to trigger activity.

REFERENCES

Arfmann, H. A., Labitzke, R., & Wagner, K. G. (1977) *Biopolymers 16*, 1815−1826.

Beschiaschvili, G., & Seelig, J. (1990) *Biochemistry 29*, 10995−11000.

Beschiaschvili, G., & Seelig, J. (1992) *Biochemistry 31*, 10044−10053.

Blume, A. (1979) *Biochim. Biophys. Acta 557*, 32−44.

Boguslavsky, V., Rebecchi, M., Morris, A. J., Jhon, D. Y., Rhee, S. G., & McLaughlin, S. (1994) *Biochemistry 33*, 3032−3037.

Boyd, N. D., White, C. F., Cerpa, R., Kaiser, E. T., & Leeman, S. E. (1991) *Biochemistry 30*, 336−342.

Brahms, S., & Brahms, J. (1980) *J. Mol. Biol. 138*, 149−178.

Cantor, C. R., & Schimmel, P. R. (1980) in *Biophysical Chemistry*, Vol. 1, p 283, Freeman, San Francisco, CA.

Chassing, G., Convert, O., & Lavielle, S. (1986) *Eur. J. Biochem. 154*, 77−85.

Chen, Y. H., Yang, J. T. Chau, K. H. (1974) *Biochemistry 13*, 3350−3359.

Choo, L. P., Jackson, M., & Mantsch, H. H. (1994) *Biochem. J. 301*, 667−670.

Cornell, D. G., Dluhy, R. A., Briggs, M. S., McKnight, C. J., & Gierasch, L. M. (1989) *Biochemistry 28*, 2789−2797.

Demel, R. A., Geurts van Kessel, W. S. M. Zwaal, R. F. A., Roelofsen, B., & van Deenen, L. M. (1975) *Biochim. Biophys. Acta 406*, 97−107.

Duplaa, H., Convert, O., Sautereau, A.-M., Tocanne, J.-F., Chassaing, G. (1992) *Biochim. Biophys. Acta 1107*, 12−22.

Evans, R. W., Williams, M. A., & Tinoco, J. (1987) *Biochem. J. 245*, 455−462.

Folkers, K., Hakanson, R., Hörig, J., Xu, J.-C., & Leander, S. (1984) *Br. J. Pharmacol. 83*, 449−456.

Fong, T. M., Yu, H. Huang, R. R. C., & Strader, C D. (1992) *Biochemistry 31*, 11806−11811.

Fromherz, P. (1975) *Rev. Sci. Instrum. 46*, 1380−1385.

Gether, U., Johansen, T. E., Snider, R. M., Lowe, J. A., III, Emonds-Alt, X., Yokota, Y., Nakanishi, S., & Schwartz, T. W. (1993) *Regul. Pept. 46*, 49−58.

Greiner, H., E. (1985) in *Tachykinin Antagonists* (Hakanson, R., & Sundler, F., Eds.) pp 333−342, Elsevier, Amsterdam.

Hölzemann, G., Greiner, H. E., Harting, J., Barnickel, G., & Seelig, A. (1993) *Regul. Pept. 46*, 453−454.

Holladay L. A., & Puett, D. (1976) *Biopolymers 15*, 43−59.

Holladay, L. A., Rivier, J., & Puett, D. (1977) *Biochemistry 16*, 4895−4900.

Huang, R. R. C., Yu, H., Strader, C. D., & Fong, T. M. (1994) *Biochemistry 33*, 3007−3013.

Huang, R. R. C., Vicario, P. P., Strader, C. D., & Fong, T. M. (1995) *Biochemistry 34*, 10048−10055.

McLaughlin, S. (1977) *Curr. Top. Membr. Transp. 9*, 71−144.

McLaughlin, S. (1989) *Annu. Rev. Biophys. Chem. 18*, 113−136.

Michaelson, D. M., Barkai, G., & Barenholz, Y. (1983) *Biochem. J. 211*, 155−162.

Nantel, F., Rouissi, N., Rhaleb, N. E., Dion, S., Drapeau, G., & Regoli, D. (1990) *Eur. J. Pharmacol. 179*, 457−462.

Nicoll, R. A., Schenker, C., & Leeman, S. E. (1980) *Annu. Rev. Neurosci. 3*, 227−268.

Ptitsyn, O. B., & Finkelstein, A. V. (1983) *Biopolymers 22*, 15−25.

Regoli, D., Dion, S., Rhaleb, N.-E., Rouissi, N., Tousignant, C., Jukic, D., d'Orleans-Juste, P., & Drapeau, G. (1989) *Biopolymers 28*, 81−90.

Regoli, D., Boudon, A., & Fauchère, J. L. (1994) *Pharmacol. Rev. 46*, 551−599.

Richards, F. (1977) *Annu. Rev. Biophys. Bioeng. 6*, 151−176.

Rolka, K., Erne, D., & Schwyzer, R. (1986) *Helv. Chim. Acta 69*, 1798−1806.

Schwyzer, R. (1987) *EMBO J. 6*, 2255−2259.

Schwyzer, R. (1991) *Biopolymers 31*, 785−792.

Schwyzer, R., Erne, D., & Rolka, K. (1986) *Helv. Chim. Acta 69*, 1789−1797.

Seelig, A. (1987) *Biochim. Biophys. Acta 899*, 196−204.

Seelig, A. (1990) *Biochim. Biophys. Acta 1030*, 111−118.

Seelig A. (1992) *Biochemistry 31*, 2897−2904.

Seelig, A., & Macdonald, P. M. (1989) *Biochemistry 28*, 2490−2496.

Seelig, A., & Dölz, R. (1991) *Ann. N.Y. Acad. Sci. 632*, 468−471.

Seelig, J., Nebel, S., Ganz, P., & Bruns, C. (1993) *Biochemistry 32*, 9714−9721.

Shibata, H., Mio, M., & Tasaka, K. (1985) *Biochim. Biophys. Acta 846*, 1−7.

Taschner, N. (1992) Diploma Thesis, University of Basel, Switzerland.

Terzi, E., Hölzemann, G., & Seelig, J. (1994) *Biochemistry 33*, 7434−7441.

Terzi, E., Hölzemann, G., & Seelig, J. (1995) *J. Mol. Biol. 252*, 633−642.

Williams, R. W., & Weaver, J. L. (1990) *J. Biol. Chem. 265*, 2505−2513.

Wilson, J. C., Nielsen, K. J., McLeish, M. J., & Craik, D. J. (1994) *Biochemistry 33*, 6802−6811.

Wiseman, T., Willigston, S., Brandts, J. F., & Lung-Nau, L. (1989) *Anal. Biochem. 179*, 131−137.

BI952434Q